Cloud Publications
International Journal of Advanced Physics
2013, Volume 1, Issue 1, pp. 1-13, Article ID Sci-58

Research Article **Open Access**

Structural and Electrical Resistivity Study of Synthesized ZnO Thick Film Resistors

R.Y. Borse[1] and V.T. Salunke[2]

[1, 2] Thin and Thick Film Laboratory, Department of Electronic Science, M.S.G. College, Malegaon Camp, Malegaon, Nasik, Maharashtra, India

Correspondence should be addressed to R.Y. Borse, ratanborse@yahoo.co.in

Publication Date: 04 January 2013

Article Link: http://scientific.cloud-journals.com/index.php/IJAPhy/article/view/Sci-58

Abstract ZnO nano powder was derived from Zinc nitrate and Dextrose by using self-propagating solution combustion technique precipitation method. The nano powder of ZnO was mixed with organic vehicle (OV) consists of butyl carbitol acetate and ethyl cellulose to form a paste. The paste was screen printed on alumina substrates using nylon screen of size 355 mesh. The white thick films were fired at temperatures of 500^{o}C, 600^{o}C and 700^{o}C for 2h. The fired films were analyzed using an X-ray diffractometer (XRD) to know its crystal structure and a Scanning Electron Microscope (SEM) to know its surface morphology. Electrical resistance of the thick films was measured at various temperatures in air. The electrical resistance of the thick films decreased with increase in temperature. The purpose is to understand the effects of firing temperature on resistivity, activation energy and TCR of the thick film resistors (TFRs). It is shown that the electrical properties are found to be functions of the temperature, non-stoichiometry and grain size of the ZnO material.

Keywords *Activation Energy, Resistivity, Stoichiometry, Thick Film Resistor*

1. Introduction

In recent years, studies on synthesis, characterization, and applications of ZnO nanostructures [1–3] have been studied extensively, because ZnO nanostructures have been regarded as a promising nanomaterial in a wide range of applications like solar cells, sensors, light-emitting diodes, piezoelectric nanogenerators, field-effect transistors, and transparent electrodes [4–10]. Zinc oxide is II–VI compound semiconductor with a wide direct band gap (3.37eV at room temperature) and a hexagonal wurtzite structure (space group P63mc with cell parameters (a= 3.25 Å, c = 5.207 Å) [11]. ZnO films can be grown by many deposition techniques, such as magnetron sputtering [12], chemical vapor deposition (CVD) [13], spray pyrolysis [14], pulsed laser deposition (PLD) [15], molecular beam epitaxy (MBE) [16], sol–gel [17], and so forth. It usually exhibits (0 0 2) texture with c-axis perpendicular to the substrate due to the lower surface free energy for (0 0 2) plane [18]. Another preferred orientation is seldom reported because of its difficulty to be formed [19]. But as a novel preferred orientation, may be it will possess different properties, and bring us new applications, so it should also be investigated in recent researches of ZnO films. In general the electrical properties of thick film resistors (TFR) are functions of several factors, such as ingredients, manufacturing technique and sintering history. The main ingredients of a TFR include a conducting paste, such as an oxide powder; a dielectric phase, such as a glass powder; and an insulating substrate, such as alumina. The oxides used in TFR can be broadly classified into two groups: metallic, where the resistivity usually obeys a power-law dependence on temperature, $\rho \alpha T^n$, where $n > 0$; and semiconducting, where the resistivity usually follows an exponential law, $\rho \propto \exp(E/k_bT)$. The electrical properties of semiconducting oxides can be modified and controlled by doping and changing its temperature. Many different types of glass and substrate materials can be used; the choice of these ingredients is determined by the type of application. Alumina, porcelain, etc. are commonly used as substrates. After sintering, all ingredients in the paste form a complicated microstructure. The electrical properties as well as the conduction process (es) of TFRs are dependent on the microstructure [20].

In this work, we report on synthesis of ZnO by using self-propagating solution combustion technique precipitation method as well as their structural and electrical properties.

2. Materials and Methods

2.1. Preparation of Zinc Oxide Nano Powder

The Zinc oxide nano structured powder was prepared by self-propagating solution combustion technique [21], employing zinc nitrate and dextrose as precursors. Proper amount of zinc nitrate and dextrose are dissolved in water contained beaker and placed on a hot plate for 15 minutes as the solution dehydrates to form a deposition like gel. Then the beaker was placed in a preheated muffle furnace at 500^{o}C. The solution boils, ignites with a flame and the entire reaction was completed within 5 minutes. The powder is amorphous in nature. Then the powder was calcinated at 650^{o}C to get nanocrystalline ZnO powder. The XRD pattern of this confirms the formation of ZnO.

2.2. ZnO Thick Film Resistor Preparation

For the preparation of ZnO thick film resistors (TFRS), the inorganic to organic materials ratio was maintained as 70:30 %. In inorganic materials, the synthesized ZnO powder was used as a functional material. The ratio of active ZnO powder to permanent binder was kept as 95:5 % in 70 % part. Glass frit (70 wt. % PbO, 18 wt. % Al_2O_3, 9 wt. % SiO_2 and 3 wt. % B_2O_3) was used as a permanent binder. Organic part consist of 8 % ethyl cellulose (EC, Loba Chemicals) as a temporary binder and 92 % butyl carbitol acetate (BCA liquid, Merck, Munchen, $C_{10}H_{20}O_4$, BP 245^{o}C) as a vehicle to make the paste. The synthesized ZnO powder was weighed crushed and mixed thoroughly with glass frit as permanent binder and ethyl cellulose as a temporary binder. The mixture was then mixed with butyl carbitol acetate as a vehicle to make the paste. Butyl carbitol acetate was added drop by drop to obtain the proper viscosity and thixotropic properties of the paste. The paste was used to prepare thick films on alumina substrate by using standard screen printing technique using 140s mesh no. 355 [22]. After screen printing, the films were dried under IR-lamp for 1h and then fired at temperatures of 500^{o}C, 600^{o}C and 700^{o}C for 2h firing cycle in muffle furnace.

2.3. Characterization of ZnO Thick Film Resistor

Powder X-ray diffraction measurements of TFRs were performed using X-ray diffractometer (XRD; Miniflex Model, Rigaku, Japan) with CuKα radiation at room temperature. Surface morphology and elemental analysis was done by scanning electron microscopy [Model JEOL 6300(LA) Germany] along with EDAX (JEON, JED-2300, Germany). The thickness of the ZnO TFRs was measured by using Taylor-Hobson (Taly-step UK) system. The thickness of the films was observed uniform in the range of 20μm to 35μm. These TFR samples were used to study the structural and electrical, properties.

Herein we report tailoring of various structural and morphological changes of ZnO using dextrose as fuel combustion. The electrical resistivity measurements were carried out using the half-bridge method in the temperature range 40-400^{o}K.

3. Results

In order to understand the crystal structure and single phase purity of the ZnO powder the X-ray diffraction was performed. The X-ray diffractograms of powder is shown in Figure 1**.** It is clearly seen that powder has hexagonal wurtzite crystal structure (JCPDS 36- 1451). Particle size of the powder is 30 nm as calculated using Debye Scherrer method. The crystallinity of ZnO synthesized at 500^{o}C is quite clear from diffractogram because of the occurrence of sharp peaks at specific Bragg's angles.

3.1. XRD Analysis

The microstructure in TFRs is very complex and affected by a variety of parameters. The composition, softening point, viscosity, thermal expansion coefficient and wetting properties of the glass frit, the ratio of the size of glass particles to that of metal oxide grains and the sintering properties of the conductor material are some parameters known to affect the final microstructure of TFRs, besides the process condition (temperature and time in a defined firing cycle).

Figure 2 shows the XRD profiles of the ZnO TFRs fired at 500^{o}C, 600^{o}C and 700^{o}C temperatures prepared from synthesized ZnO powder. It is revealed that all the samples have diffraction peaks corresponding to (100), (002), (101), (102), (110), (103), (200), (112), (201) and (202) directions of the wurtzite hexagonal ZnO crystal structure [JCPDS 36- 145)] similar to Joseph et al. [23]. Some peaks of alumina substrate (indicated with X) was also found in the XRD profile of the TFRs.
The XRD pattern was used to calculate the crystallite size of ZnO by using Scherrer's formula [24].

$$D = \frac{0.9\lambda}{\beta\cos\theta} \qquad (1)$$

Where, D is the crystallite size, β is peak full width half maxima of the (101) peak of the XRD pattern, λ is wavelength of X-ray radiation (1.542 Ǻ) and θ is the diffraction angle.

Figure 3 shows the plot of FWHM, crystallite size and Interplaner spacing versus firing temperatures of ZnO thick film resistors fired at 500^{o}C, 600^{o}C and 700^{o}C.

3.2. Scanning Electron Microscopy (SEM) Analysis

Figure 4 shows the SEM images of synthesized ZnO thick film resistors fired at 500, 600 and 700^{o}C. All the SEM images are recorded at 50k magnification for comparison. From the SEM images it is seen that all the films are porous with small grains (sub-micron). The films fired at 500 and 600^{o}C are more porous as compared to film fired at 700^{o}C. The grain size is little bit larger as the increase of firing temperature although the increase is not significant.

3.3. Elemental Analysis (EDAX Analysis)

Figure 5 shows the EDAX spectra of ZnO TFRs fired at different temperatures. The EDAX analysis shows presence of only Zn and O as expected, no other impurity elements were present in the ZnO thick films The mass percentage of Zn was found to increase with an increase of the firing temperature due to release of excess oxygen.

3.4. Electrical Characterization

The electrical Resistivity, as a function of temperature, for all the samples fired at 500,600 and 700°C is shown in Figure 6. All samples show semiconducting behavior. It is clear from the plots that the resistivity at room temperature is decreasing with firing temperature. The electrical resistance of ZnO TFRs is plotted as *log R* versus 1/T in Figure 7. From Figure 7, one may also notice that there are two nearly linear regions of conduction with different activation energies, one for higher and one for the lower temperature region. The change from one region to the other is not sharp but it is a gradual one. The activation energies were calculated for the studied samples. Two separate activation energies may be noticed for the samples that presented a significant apparent porosity, the higher activation energies being predominated at high temperatures, while the lower ones at lower temperatures. It is our basic conclusion that in the 50- 400°K temperature range, the obtained values for the activation energies may be assigned to a different conduction mechanism, due to the migration of charge carriers in the presence of pores.

Temperature coefficient of resistance (TCR) of ZnO TFRs fired at 500, 600 and 700°C is calculated by using the following relation,

$$\mathrm{TCR} = \frac{1}{R_o}\left(\frac{\Delta R}{\Delta T}\right) \ /^{O}\mathrm{K} \qquad (2)$$

Temperature coefficient of resistance of ZnO TFR deposits is negative for all samples, indicating semiconducting behavior.

Figure 8 shows the variation of TCR with operating temperature of the ZnO TFRs. It is found that TCR is negative and its value decreased gradually with increase of operating temperature.

The variation of resistivity, TCR and activation energy of the ZnO TFRs fired at 500, 600 and 700°C is summarized in Table 2.

Table 2: *Resistivity, Activation Energy and TCR with Firing Temperature of ZnO TFRs*

Firing Temperature, °C	**Crystallite size, nm**	**Resistivity, (ρx10^5) Ω-cm**	**Activation Energy(eV)**		**TCR, /°C**
			Lower temp.	**Higher temp.**	
500	46.48	4.26	0.0045	0.1279	2.3061
600	51.47	1.06	0.003782	0.1212	0.009365
700	53.39	0.71	0.001046	0.08046	0.005005

4. Discussion

From the XRD profiles of the ZnO TFRs fired at different temperatures, it is revealed that all the samples have diffraction peaks corresponding to (100), (002), (101), (102), (110), (103), (200), (112), (201) and (202) directions of the wurtzite hexagonal ZnO crystal structure [JCPDS 36- 145)]. Some peaks of alumina substrate (indicated with X) was also found in the XRD profile of the TFRs. It has been observed that (101) reflections are of maximum intensity, which indicates that ZnO TFRs have preferred orientation in the (101) plane, the intensity of which increasing with increase in firing temperature of the TFR. The higher peak intensities of an XRD pattern is due to the better crystallinity and bigger grain size can be attributed to the agglomeration of particles. Crystalline nature increases as firing temperature increased to 700°C. This is clear from the increase in peak intensity. Also in the present case the increase in Zn content and firing temperature is the reason for high preferential orientation along the (101) plane. A high degree of crystal orientation reduces the probability of the scattering of the carriers at the grain boundary.

The average crystallite size of ZnO TFRs fired at 500, 600, and 700ºC calculated by Scherrer's formula was observed as 46.48, 51.47 and 53.39nm respectively. It has been observed that the crystallite size increases with increase in firing temperature. The bigger grain size can be attributed to the agglomeration of particles due to increase in firing temperature [25, 26, 27]. The XRD patterns of all the films seem to be qualitatively similar. Upon increasing the firing temperature from 500 to 700°C, the 2θ increases and the FWHM value decreases, indicating that the (101) spacing decreases and the crystallinity (crystalline size) of the ZnO TFR is improved with increasing firing temperature as indicated in Figure 3 (a). These results are thought to be related to the reduction in oxygen atoms due to higher firing temperature. This change influences the stoichiometry of ZnO TFRs. The interplanar spacing of (101) plane is therefore 2.4797, 2.479 and 2.4777nm for the TFRs fired at 500, 600, and 700ºC respectively (Figure 3(b)), which is in good agreement with the standard value 2.4759nm shown by JCPDS card 36-1451 file data.

The SEM images of synthesized ZnO thick film resistors fired at 500, 600 and 700°C and recorded at 50k magnification showed that, the material is characterized by some intergranular porosity. Some large open pores of several micrometers in diameter and small open pores of several tens of nanometers in diameter are present in samples. Agglomeration of small crystallites also seems to be present in the certain region. The contrast difference is due to different orientations of the crystallites. The grain size is little bit larger as the increase of firing temperature although the increase is not significant.

At 500°C firing temperatures the surface morphology of the ZnO TFR showed individual grains clearly and the grain size enlarged above firing temperature of 500°C. Figure 4 (c) shows formation of submicrometer crystallites distributed more or less uniformly over the surface with very small number of open pores and several particles connected with each other. The particle size of ZnO TFR fired at 700°C is more than other TFRs. As firing temperature is increased, the particle size increases. As seen from SEM images, the particles size increases with the firing temperature. The number of particles which has hexagonal structure increased with increasing firing temperature. The number of voids observed is more for the ZnO TFRs fired at 500°C and 600°C.

The EDAX analysis shows presence of only Zn and O as expected, no other impurity elements were present in the ZnO thick films. The mass percentage of Zn was found to increase with an increase of the firing temperature due to release of excess oxygen [28]. It was found that the ZnO films are non-stoichiometric. The deficiency or excess of any type of atom in the crystal results in a distorted band structure, with a corresponding increase in conductivity. Zinc oxide loses oxygen on heating so that zinc is then in excess. The oxygen, of course, evolves as an electrically neutral substance so that it is associated with each excess zinc ions in the crystal. There will be two electrons that remain trapped in the solid material, thus leading to non-stoichiometricity in the solid. This leads to the formation of the n-type semiconductor [29]. Table 1 gives quantitative elemental analysis of ZnO thick films**.** It is clear from the table that with increasing firing temperature the mass % of oxygen decreases

Table 1: *Composition of the ZnO Thick Films at Different Firing Temperature*

Firing Temperature	Element	At. Wt. %	Mass %
500°C	Zn	77.33	93.47
	O	22.67	6.53
600°C	Zn	79.67	94.12
	O	20.33	5.88
700°C	Zn	80.39	94.37
	O	19.61	5.63

The electrical Resistivity, as a function of temperature, for all the samples fired at 500,600 and 700^{o}C show semiconducting behavior. It is clear from the plots that the resistivity at room temperature is decreasing with firing temperature. Generally, at higher temperatures, the carriers are thermally activated to extend states with higher mobility. In order to examine the electrical conduction mechanism of ZnO TFRs $\rho_{(T)}$ is compared to

$$\rho = \rho_0 \exp (\Delta E/ k_B T) \qquad (3)$$

which represents simple thermally activated electrical conductivity [30], where an electron or hole (as the charge carrier) moves from one localized state to another due to an exchange of energy between the charge carrier and phonon (the localization is not a consequence of interaction with a phonon, but could occur due to a random electric field or disordered arrangement of atoms). In Eq. (3), ρ_o is the electrical resistivity at extremely high temperatures, ΔE is the thermal activation energy (or simple activation energy) of the electron or hole, and K_B is the Boltzmann constant. Realizing that the TFRs are polycrystalline, only general statements will be made here regarding the electrical conduction mechanism. It is well established that the firing temperature in the ZnO TFRs, which consequently decreases the energy gap and hence the resistivity of the material.

The variation *log R* versus 1/T for ZnO TFRs is shown in Figure 7 does not exhibit linear behavior through the entire temperature range; we conclude that Eq. (3) is an inadequate description. However, this equation can provide a rough idea of thermal activation energies in narrow temperature regions where the data can be fitted. The two distinct linear regions in *log R* versus 1/T curve for ZnO films revealing two activation energies, one for higher temperature region and other for lower temperature region. The activation energy in the lower temperature region is always less than the energy in the higher temperature region because material passes from one conduction mechanism to another [31].

In low temperature region, the increase in conductivity is due to the mobility of charge carriers which is dependent on the defect/dislocation concentration. So, the conduction mechanism is usually called the region of low temperature conduction. In this region activation energy decreases, because a small thermal energy is quite sufficient for the activation of the charge carriers to take part in conduction process. In other words the vacancies/ defects weakly attached in lattice can easily migrate (extrinsic migration). Hence increase in the conductivity in the lower temperature region can be attributed to the increase in charge mobility.

In high temperature region, the activation energy is higher than that of low temperature region. In this region the electrical conductivity is mainly determined by the intrinsic defects and hence is called high temperature or intrinsic conduction. The high values of activation energy obtained for this region may be attributed to the fact that the energy needed to form defects much larger than the energy required for its drift. For this reason the intrinsic defects caused by the thermal fluctuations determine the electrical conductance of the film samples only at elevated temperature [31].

The activation energies were calculated for the studied samples. Two separate activation energies may be noticed for the samples that presented a significant apparent porosity, the higher activation energies being predominated at high temperatures, while the lower ones at lower temperatures. It is our basic conclusion that in the 50 - 400^{o}K temperature range, the obtained values for the activation energies, may be assigned to a different conduction mechanism, due to the migration of charge carriers in the presence of pores. Temperature coefficient of resistance of ZnO TFR deposits is negative for all samples, indicating semiconducting behavior. Figure 8 shows the variation of TCR with operating temperature of the ZnO TFRs. It is found that TCR is negative and its value decreased gradually with increase of operating temperature, which suggests an electron emission process which always improves with rise in temperature. The decrease in TCR value with increase in firing temperature may be attributed to increase in the degree of crystallinity and grain size [32, 33].

5. Conclusion

Single-phase polycrystalline ZnO have been prepared using the screen printing method. The structural analysis (XRD) of all ZnO TFRs suggests the increase in crystallite size on increasing firing temperature. XRD and SEM studies have revealed polycrystalline structure of ZnO thick film resistors. It also shows voids between the particles basically due to evaporation of the organic solvent during the firing of the films. Electrical resistivity measurements reveal semiconducting behavior for all TFRs, while their resistivity values decrease with increase in firing temperature due to decrease in energy gap. It is found that the films fired at 700°C offer low resistivity, low activation energy, low TCR and high crystallite size can used to fabricate resistive components and used in gas sensor applications.

Figures

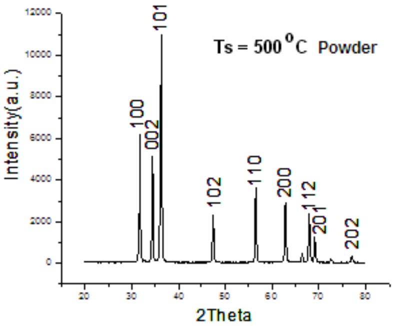

Figure 1: *XRD profile of synthesized ZnO powder*

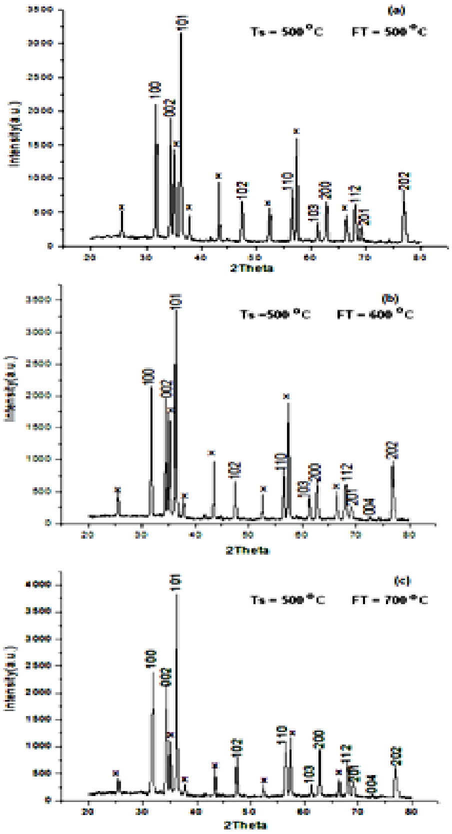

Figure 2: *X-ray diffraction patterns of ZnO TFRs fired at (a) 500°C, (b) 600°C and (c) 700°C*

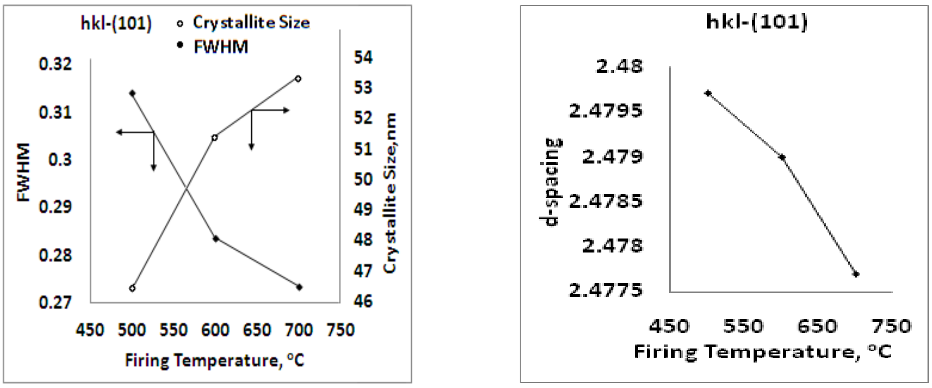

(a) FWHM and crystallite size

(b) Interplaner spacing

Figure 3: *Plot of (a) FWHM, crystallite size and (b) Interplaner spacing versus firing temperature*

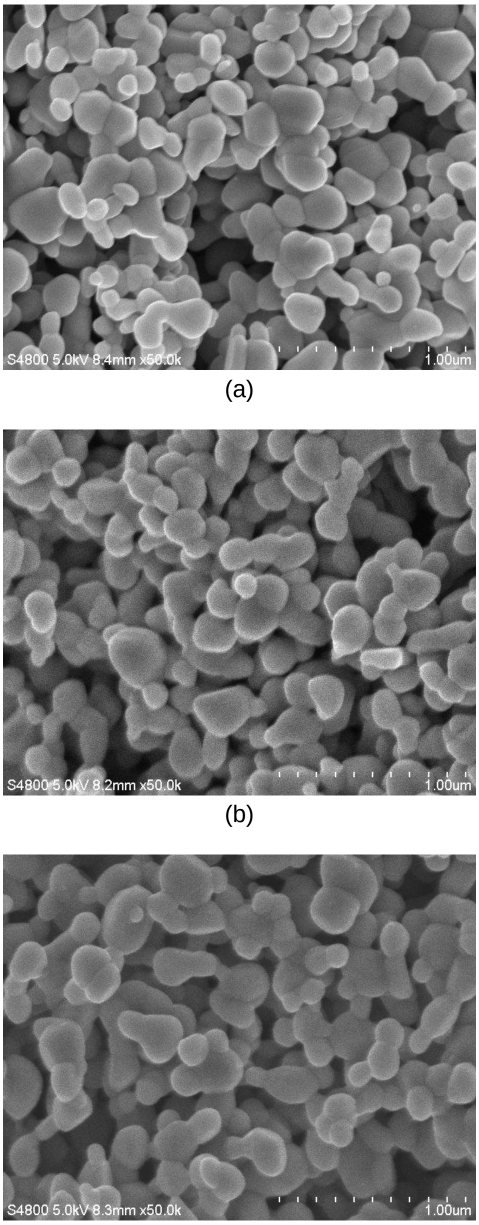

(c)

Figure 4: *SEM images of synthesized ZnO TFRs fired at (a) 500, (b) 600 and (c) 700^{o}C*

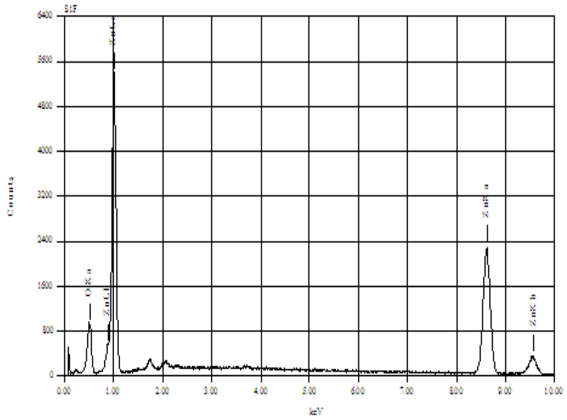

(a) EDAX spectra of ZnO thick film fired at 500^{o}C

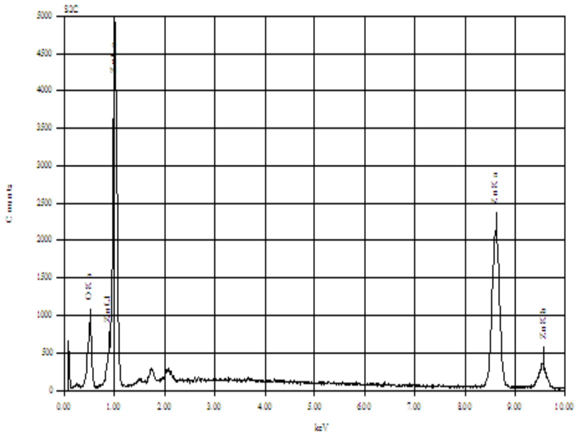

(b) EDAX spectra of ZnO thick film fired at 600^{o}C

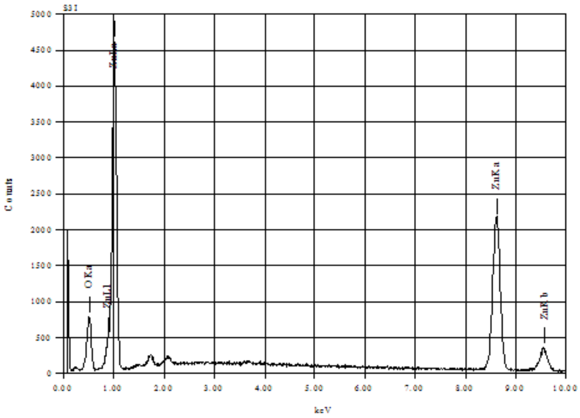

(c) EDAX Spectra of ZnO thick film fired at 700^{o}C

Figure 5: *EDAX Spectra of ZnO TFRs fired at (a) 500, (b) 600 and (c) 700^{o}C*

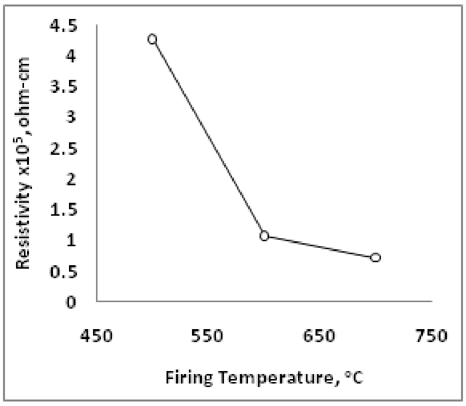

Figure 6: *Resistivity versus firing temperature*

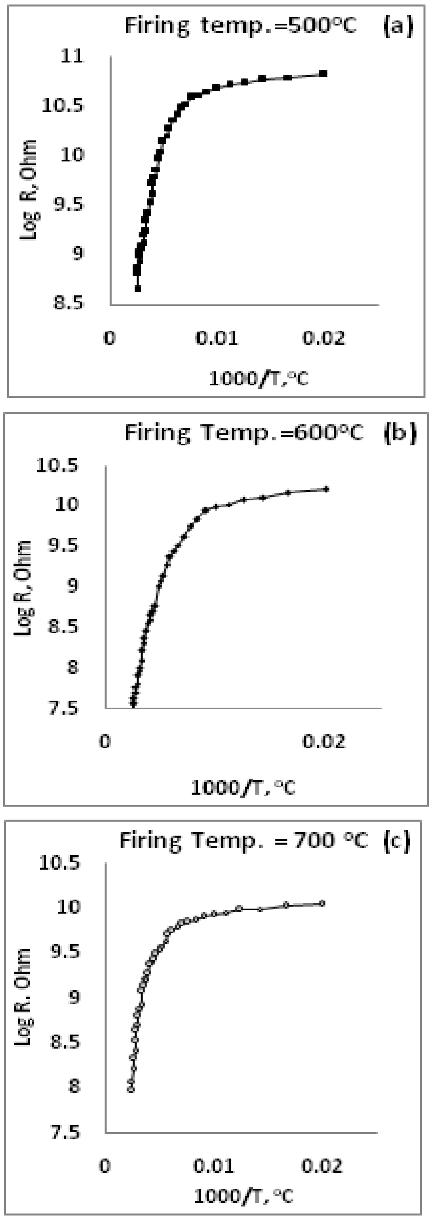

Figure 7: *Plot of Log R versus (1/T) for ZnO TFRs fired at (a) 500, (b) 600 and (c) 700^{o}C*

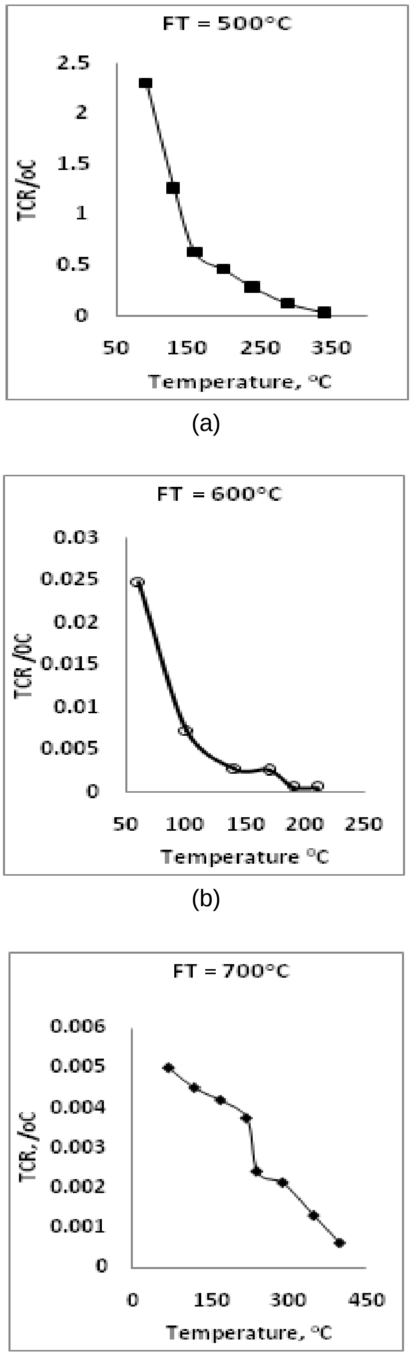

(a)

(b)

(c)

Figure 8: *Plot of TCR versus operating temperature of ZnO TFRs at (a) 500, (b) 600 (c) 700*^{o}*C*

Acknowledgement

The author is pleased to acknowledge the UGC for providing grants for minor research project, management authorities of M.G. Vidyamandir, Malegaon camp, Dist:-Nashik (MS) India for kind support, Principal, M.S.G. College, Malegaon, Nashik, for providing all the required infrastructural facilities for doing this work, Department of Physics, University of Pune for providing XRD results and NCL, Pune, India for providing SEM results.

References

[1] Z.L. Wang. Materialstoday. 2004. *7*; 26-33.

[2] W.I. Park et al. Adv. Mater. 2002. 14; 1841.

[3] P.X. Gao et al. Adv. Funct. Mater. 2006. 16; 53.
[4] J.E. Beek et al. Adv. Mater. 2004. 1216.

[5] Z.L. Wang et al. Science. 2006. 312; 242.

[6] J. Goldberger et al. J. Phys. Chem. 2005, B 109; 9.

[7] J.K. Sheu et al. J. Tune, Appl. Phys. Lett. 2007. 90; 263511.

[8] Z. Zhang et al. Nano Lett. 2008. 8; 652.

[9] Y.Y. Noh et al. Appl. Phys. Lett. 2007. 91; 043109.

[10] Y.F. Hsu et al. J. Appl. Phys. 2008. 103; 083114.

[11] V. Srikant et al. J. Appl. Phys. 1998. 83; 5447.

[12] Z.Z. Ye et al. Chinese J. Semicond. 2001. 22; 1015 (in Chinese).

[13] B.M. Ataev et al. Mater. Sci. Eng. 1999. B 65; 159.

[14] F. Paraguay. Thin Solid Films. 1999. 350; 192.

[15] M. Joseph et al. Physica. 2001. B 302-303; 140.

[16] Z.K. Tang. Appl. Phys. Lett. 1998. 72; 3270.

[17] A.E. Jime´nez-Gonza´lez. J. Cryst. Growth. 1998. 192; 430.

[18] N. Fujimura. J. Cryst. Growth. 1993. 130; 269.

[19] N.H. Tran et al. J. Phys. Chem. 1999. B 103; 4264.

[20] K.M. Anisur Rahman. *Hopping and Ionic Conduction in Ti Oxide –Based Thick Film Resistor Compositions*. J. Am. Ceram. Soc. 1997. 80 (5) 1198-1202.

[21] M. Jayalakshmi. *Single Step Solution Combustion Synthesis of ZnO/Carbon Composite and Its Electrochemical Characterization for Supercapacitor Application.* Int. J. Electrochem.Sci. 2008. 3; 96-103.

[22] S.C. Kulkarni et al. Study on Gas Sensing Performance of In_2O_3 Thick Film Resistors Prepared by Screen Printing Technique. Sensors & Transducers Journal. 2011. 125 (2) 194-204.

[23] B. Joseph Bull. Mater. Sci.1999. 22.

[24] B.D. Cullity. Elements of X-ray Diffraction (Addison- Wesley Publishing Co.) 1056.

[25] Preetam Singh. Bull.Mater. Sci. 2008. 31 (3) 573-577.

[26] Yong Jae Kwon. J.of Ceram.Proc. Res. 2002. 3; 146.

[27] B.K. Karunagaran. Cryst. Res. Technol. 2002. 37 (12) 1285-1292.

[28] E. San Andress. Vac. Sci.Tech. 2005 23 (6) 1523-1530.

[29] Devidas Ramrao. IEEE Sensors Journal. 2007. 7 (3) 434-439.

[30] V.A. Patakova. Phys. Stat. Sol. 1972. 12; 623.

[31] I.S. Ahmed Frag. Indian J. Pure and Appl. Phys. 2005. 43; 446.

[32] Tamborin M et al. *Piezoresistive Properties of RuO2-based Thick-Film Resistors: The Effect of RuO2 Grain Size.* Sensors and Actuators A. 1997. 58; 159-64.

[33] Sonia Vionnet Menot, 2005: *Low Firing Temperature Thick-Film Piezo Resistive Composites-Properties and Conduction Mechanism.* University de Franche-Comte, Besancon, France, 3290.